

# Hydrogeology and grouting - a field experiment in shallow, crystalline rock

Åsa Fransson

*Department of Earth Sciences, University of Gothenburg, Gothenburg, Sweden*

**ABSTRACT:** When constructing a tunnel or a shaft in a fractured rock mass, the main water-bearing features are of major importance. A limited reduction in leakage, as well as a greater impact area, are potential consequences if these features are not considered in hydrogeological descriptions and in grouting design. This paper presents a grouting field experiment performed in a shallow, crystalline rock mass. An experiment where the spatial distribution of hydraulic conductivity (transmissivity) of water-bearing features was expected to show both directional dependence and connectivity. This was confirmed, grouting was performed, and hydraulic conductivity reduced. We expect that the demonstrated experimental work, highlighting general nature, pattern, and properties, can be used to improve hydrogeological descriptions and grouting design and form a basis for environmental impact assessments. Further, storage coefficient, and hydraulic aperture, based on transmissivity, can, potentially, be an additional indicator of fracture stiffness and situation of stress.

*Keywords: Hydrogeology, grouting, environmental impact, transmissivity, storage coefficient, fracture stiffness.*

## 1 INTRODUCTION

General nature, e.g., stratigraphy of soil or features in rock, the resulting geometrical pattern, and hydraulic properties, are key for grouting design and environmental impact assessments. Impact areas, with changes in head, may, for example, result in settlement of soil and damage to constructions. Since the same type of data can be used both for grouting design and as a basis for environmental impact assessments, more attention should be given to this double value of hydrogeological descriptions and the related data.

This paper presents a grouting field experiment performed in a shallow, crystalline rock mass within the Varberg tunnel project. The Varberg tunnel project includes the construction of a double track railway where the main tunnel and a service tunnel are built in rock and open troughs intersect both soil and rock. Focus for the field experiment were engineering feasibility and hydraulic efficiency, investigating spatial distribution of hydraulic conductivity (transmissivity) of main water-bearing features. Key aspects to address were connectivity, anisotropy, and heterogeneity.

## 2 GEOLOGICAL SETTING

The bedrock of Varberg is dominated by crystalline rocks, Figure 1. The main rock types are charnockite (green-brown) and gneiss (pink). The experiment was performed in a rock volume consisting of charnockite and in the area indicated by the black circle, Figure 1. A photograph of the site and an illustration of the geometry of the experiment are presented in Figure 2. The photo shows the rock surface, a partial cover of soil and boreholes for transient, time-dependent, hydraulic testing.

The main water-bearing features were expected to be directionally dependent, i.e., horizontal, and interconnected (large).



Figure 1. Bedrock map showing the Varberg area and the location of experiment (black circle). Main rock types: charnockite (green-brown) and gneiss – granitic, dioritic (pink), (Swedish Geological Survey 2023).

## 3 MATERIAL AND METHODS

Data for the hydrogeological description, for grouting design, and for follow up, originated from one transient, time-dependent, hydraulic test, short duration water loss measurements (WLM), and measurements of grout take. The latter two for two grouting rounds. All grouting boreholes were vertical focusing on the main water-bearing features that were expected to be horizontal.

A stepwise procedure was used to perform the experiment, starting with the drilling of five boreholes, see blue circles in Figure 2 (right) and within white frames in the photo (left). Transient hydraulic testing of one of these boreholes allowed monitoring of groundwater levels for the other boreholes, thus investigating whether the boreholes were interconnected. The next step was drilling of the first round of grouting boreholes, black filled circles, Figure 2. Subsequently, water loss measurements were performed, and the boreholes were grouted. Finally, the same procedure was repeated for the second grouting round. This can be referred to as a split-spacing procedure.

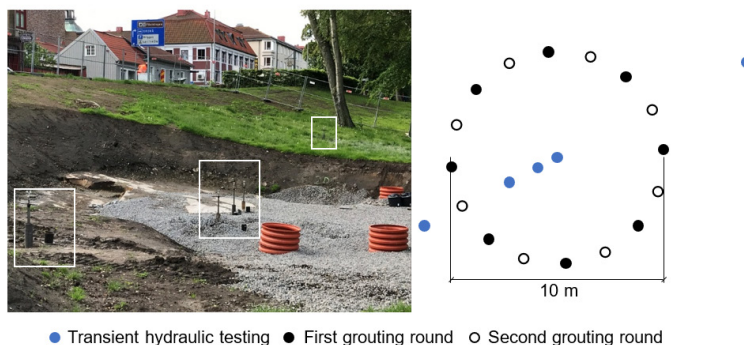


Figure 2. Geometry of field experiment. Boreholes for transient hydraulic testing, blue filled circles to the right and shown within white frames in the photograph to the left. Boreholes for water loss measurements and grouting, first round - black, filled circles, second round - black, unfilled circles.

### 3.1 Hydraulic testing

Water loss measurements using several boreholes aimed at reflecting the spatial distribution of hydraulic properties e.g., hydraulic conductivity,  $K$  or transmissivity,  $T$ . Further, transient hydraulic testing was performed to indicate connectivity and anisotropy. The latter was also used for evaluation of a storage coefficient,  $S$ . A parameter that can be related to fracture (normal) stiffness,  $k_n$ .

#### 3.1.1 Transient hydraulic testing

A test procedure where pressure is registered as a function of time is described as a transient, time-dependent, test. The evaluation of the transient data was performed based on Cooper & Jacob (1946) resulting in a transmissivity,  $T$  and a storage coefficient,  $S$ . The transmissivity reflecting the ability of a fracture (or formation) to transmit water and the storage coefficient reflecting its ability to store or emit water. The latter can be expressed:

$$S = \rho_f g (1/k_n + eC_f) \quad (1)$$

where  $e$  is the fracture (void) aperture and  $C_f$  the fluid compressibility, see e.g. Doe & Geier (1990). When  $eC_f$  is small compared to  $1/k_n$ , the storage coefficient can be described as inversely proportional to the (normal) stiffness of the fracture.

Since the water pressure was artesian, above the rock surface, a value of the head, was obtained by initially measuring pressure using a packer and a pressure gauge. After this, the packer was opened and a flow,  $Q$ , was measured.

When the packer was opened and the pressure lowered, pressure responses were noted in the surrounding four boreholes, indicating a well-connected water-bearing formation. The three boreholes closest to the tested borehole showed a very fast pressure response.

#### 3.1.2 Water loss measurements (WLM)

Water loss measurements were performed measuring the pumped volume of water for five minutes and at a pressure of 3 bars. Based on this data specific capacity,  $Q/dh$ , and hydraulic aperture,  $b_{hyd}$ , were estimated. Specific capacity was assumed to be approximately equal to the transmissivity,  $T$ :

$$\frac{Q}{dh} \approx T = \frac{\rho_f g b_{hyd}^3}{12\mu_f} \quad (2)$$

The right-hand side of the equation is referred to as the cubic law (Witherspoon et al. 1980) and assumes one, individual, and planar fracture. The equation includes density of fluid (water),  $\rho_f$ , gravity,  $g$ , and the viscosity of the fluid,  $\mu_f$ .

### 3.2 Grouting

Grouting was performed using a cement-based grout and a grouting pressure of 5 bars. Grouting time was set to 15 minutes and the maximum allowed volume (grout take) to 100 liters per borehole (including borehole volume). For some boreholes this was increased to 150 liters. The selected grout, *Injektering 30*, has a grain-size distribution with a  $d_{95}$  of 30  $\mu\text{m}$ . As a principle, simplified, guideline, the fracture aperture should be greater than three times the  $d_{95}$  of the material i.e.,  $3 \cdot 30 = 90 \mu\text{m}$  (e.g., Martinet 1998).

Based on Equation 2, the specific capacity,  $Q/dh$ , would be  $4.6\text{E-}7 \text{ m}^2/\text{s}$  if using an aperture of 90  $\mu\text{m}$ , a density of water,  $\rho_f$ , of  $1000 \text{ kg/m}^3$ , a gravity,  $g$ , of  $9.81 \text{ m/s}^2$  and a viscosity of water,  $\mu_f$ , of  $1.3\text{E-}3 \text{ Pas}$ . This would correspond to a water loss of approximately 4 liters (for 5 minutes and at 3 bars,  $5 \cdot 60 \cdot 1000 \cdot 30 \cdot 4.6\text{E-}7$ ). Boreholes with water losses exceeding 4 liters have potential to be groutable with the selected grout.

## 4 RESULTS AND DISCUSSION

Three topics are of main interest in the discussion below: Main water-bearing features – spatial distribution of hydraulic properties; Grouting results based on hydraulic testing; and Hydromechanics based on hydraulic testing.

### 4.1 Main water-bearing features – spatial distribution of hydraulic properties

The transient, time-dependent, testing of one of the (blue) boreholes, Figure 2, allowed monitoring of groundwater levels for the other (blue) boreholes. Lowering of levels confirmed the boreholes being *interconnected*. In addition, the artesian pressure indicated a low vertical conductivity, with overflow at the borehole casing rather than a fast pressure reduction due to vertical fracture flow. In terms of *anisotropy*, the horizontal (or sub-horizontal) water-bearing properties therefore exceeded the vertical.

A final issue to address was the *heterogeneity* of the expected, and confirmed, sub-horizontal feature(s). Table 1 presents water loss measurements and grout take for the eight boreholes included in the first grouting round (black, filled circles, Figure 2). Similar water losses were found, all within 21 to 25 liters, for 5 minutes and 3 bars, indicating a homogeneous, open, structure. If using Equation 2 and assuming one, individual fracture, the hydraulic aperture would vary between 155 to 164  $\mu\text{m}$ , see Table 1.

Table 1. First grouting round. Water loss measurements, WLM, were performed at 3 bars and the volume for 5 minutes was documented. Grout take included borehole filling. Packers for WLM installed at 0.5m, for grouting at 1.5m.

Borehole	Length, $L$ [m]	$WLM_{5min, 3bar}$ [liters]	$Q/dh$ [m <sup>2</sup> /s]	$Q/dh/L$ [m/s]	$b_{hyd}$ [ $\mu\text{m}$ ]	Grout take [liters]
3A	9.2	22	2.4E-6	2.8E-07	157	150
3B	9.0	21	2.3E-6	2.7E-07	155	150
3C	9.1	22	2.4E-6	2.8E-07	157	100
3D	9.1	21	2.3E-6	2.7E-07	155	100
3E	9.2	25	2.8E-6	3.2E-07	164	100
3F	9.2	23	2.6E-6	2.9E-07	160	100
3G	9.1	24	2.7E-6	3.1E-07	162	150
3H	9.3	22	2.4E-6	2.8E-07	157	150

Table 2. Second grouting round. Water loss measurements were performed at 3 bars and the volume for 5 minutes was documented. Grout take excluding borehole filling found within parenthesis. Packers for WLM installed at 0.5m, for grouting at 1.5m.\*For WLM packer installed at 6 m.

Borehole	Length, $L$ [m]	$WLM_{5min, 3bar}$ [liters]	$Q/dh$ [m <sup>2</sup> /s]	$Q/dh/L$ [m/s]	$b_{hyd}$ [ $\mu\text{m}$ ]	Grout take [liters]
4A	14	0	0	0	0	115 (73)
4B	14	3	3.3E-7	2.5E-08	81	70 (28)
4C	14	0	0	0	0	42 (0)
4D	14	2	2.2E-7	1.6E-08	71	117 (75)
4E	14	36	4.0E-6	3.0E-07	185	42 (0)
4F	14	0*	0	0	0	missing
4G	14	0	0	0	0	42 (0)
4H	14	0	0	0	0	42 (0)

## 4.2 Grouting results based on hydraulic testing

Before the first grouting round, the hydraulic apertures exceeded  $90\ \mu\text{m}$  (or 4 liters for 5 min and 3 bars), see Table 1 and Figure 3 (left). The water-bearing feature was therefore expected to be groutable with the selected cement-based grout. This was confirmed by the grout take since the maximum allowed volume was used for all boreholes of the first grouting round, see Table 1.

Based on hydraulic testing, the grouting result was good. Prior to the first grouting round, all water loss measurements were between 21 and 25 liters, see Table 1. Following the first grouting round and before the second, all losses except for one were below 4 liters or  $90\ \mu\text{m}$  (green boreholes, Figure 3, right). In addition, grout take was below the maximum allowed volume for all boreholes of the second grouting round with no or limited grout take for most boreholes.

The first grouting round was performed for one lower level, 9-18 m, and one upper level, 1.5-9 m. For the lower level, below 9 meters, there were no (low) documented water losses and grout takes for the boreholes (except for one where data was missing). Therefore, the boreholes of the second grouting round, Table 2, being 14 m deep instead of 9 m was not expected to influence the result.

Drilling of additional boreholes for control, and if needed, grouting, close to the borehole indicated by red colour in Figure 3 would have been possible, this was not performed for this experiment.

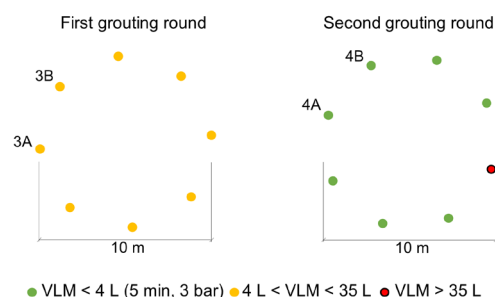


Figure 3. Water loss measurements (WLM). Orange or red colour indicate a possibility that the boreholes are groutable with the cement-based grout ( $VLM > 4$  liters or  $b_{hyd} > 90\ \mu\text{m}$ ). Green - a reduction in water loss.

## 4.3 Hydromechanics based on hydraulic testing

The transient hydraulic test resulted in a transmissivity of  $3.8\text{E-}6\ \text{m}^2/\text{s}$ , a hydraulic aperture of about  $180\ \mu\text{m}$ , close to the apertures in Table 1, and a storage coefficient of  $3.5\text{E-}4$ . The storage coefficient reflecting the ability of the formation to store or emit water. In simple terms, and as described by Equation 1, the storage coefficient can be assumed being inversely proportional to the stiffness of a fracture, where a good ability to store water, a high storage coefficient, would correspond to a low stiffness. In Olsson & Barton (2001), experimental data show that for smooth walls or very wide apertures the mechanical aperture and the theoretical smooth wall conducting aperture are equal. The homogeneity of the investigated feature, all hydraulic apertures,  $b_{hyd}$ , being within a small range, Table 1, increases the likelihood of an open fracture and the mechanical and hydraulic aperture being of the same size. Estimating a stiffness using Equation 1 and the storage coefficient,  $S$ , of  $3.5\text{E-}4$ , would result in a stiffness of  $0.03\ \text{GPa/m}$ . This is low, even compared to e.g., Guglielmi et al. (2008) that included an example of stiffness in the order of  $1\ \text{GPa/m}$  at low effective stress,  $< 0.5\ \text{MPa}$ . A stiffness as low as  $0.03\ \text{GPa/m}$ , may serve as an indication that the effective stress is low, close to zero or even tensile as suggested by a stiffness to hydraulic aperture relationship presented in Fransson (2014). A paper that also includes data from Guglielmi et al. (2008).

The investigated boreholes partially intersected the rock volume where the entrance to the service tunnel was later excavated, see Figure 4. The photograph shows the excavation and confirms the presence of the shallow, (sub)horizontal and large fractures expected based on the field experiment. A low stiffness, as estimated here based on the storage coefficient, is reasonable given the shallow depth. Pointing at a low (no) compressive stress and a procedure (above) for hydraulic testing, evaluation, and indication of stress. A low grouting pressure is likely to reduce the risk of jacking.



Figure 4. The boreholes of the experiment, Figure 2, partially intersected the rock volume where the entrance to the service tunnel was later excavated. The shallow, (sub)horizontal and large fractures are visible.

## 5 CONCLUSIONS

The experiment was focused on engineering feasibility and hydraulic efficiency. The spatial distribution of hydraulic properties of the main water-bearing feature(s) pointed at a well-connected, homogeneous fracture and an anisotropic rock mass (high horizontal hydraulic conductivity compared to vertical). The fracture was, as expected, groutable with a cement-based grout and the hydraulic conductivity was reduced. The demonstrated experimental work, can be used to improve hydrogeological descriptions and grouting design, and form a basis for environmental impact assessments. Further, storage coefficient, and hydraulic aperture, based on transmissivity, can, potentially, be an additional indicator of fracture stiffness and situation of stress.

## ACKNOWLEDGEMENTS

The author would like to thank the Swedish Transport Administration (Trafikverket) and Implenia Sverige AB for the experimental data. Special thanks go to Erika Lindqvist and Hannes Wiklund for their help in performing hydraulic tests. Financial support provided by the Swedish research council, Formas, and the Rock Engineering Research Foundation, BeFo, are also greatly appreciated.

## REFERENCES

- Cooper Jr, H. H., & Jacob, C. E. 1946. A generalized graphical method for evaluating formation constants and summarizing well-field history. *Eos, Transactions American Geophysical Union* 27(4), 526-534.
- Doe, T. W., & Geier, J. E. 1990. Interpretation of fracture system geometry using well test data (No. STRIPA-TR-91-03). Swedish Nuclear Fuel and Waste Management Co.
- Fransson, Å. 2014. The use of basic models to explain in situ hydraulic and hydromechanical tests in fractured rock. *International Journal of Rock Mechanics and Mining Sciences* 69, 105-110.
- Guglielmi, Y., Cappa, F., Virieux, J., Rutqvist, J., Tsang, C. F., & Thoraval, A. 2008, June. A new in-situ approach for hydromechanical characterization of mesoscale fractures: the High-Pulse Poroelasticity Protocol (HPPP). In: *Proceedings of the 42nd U.S. Rock Mechanics Symposium/2nd US-Canada RockMechanics Symposium*, San Francisco, ARMA 08-214, pp. 1-7, A. A.Balkema Publishers.
- Martinet, P. 1998. *Flow and clogging mechanisms in porous media with applications to dams*. Doctoral thesis, Royal Institute of Technology, Stockholm, Sweden.
- Olsson, R., & Barton, N. 2001. An improved model for hydromechanical coupling during shearing of rock joints. *International journal of rock mechanics and mining sciences* 38(3), 317-329.
- Swedish Geological Survey. 2023. Berggrund (bedrock) 1:50000 - 1:250000. Retrieved February 21, 2023, from <https://apps.sgu.se/kartvisare/>
- Witherspoon, P. A., Wang, J. S., Iwai, K., & Gale, J. E. 1980. Validity of cubic law for fluid flow in a deformable rock fracture. *Water resources research* 16(6), 1016-1024.